

Investigation of a Polar Mesospheric Cloud Front in the Southern Hemisphere: Influence of Temperature Inversion Layers and Gravity Waves



Aklima Khatun, Brentha Thurairajah
Virginia Tech, Department of Electrical and Computer Engineering

1. Introduction

- Polar Mesospheric Clouds (PMCs) are high-altitude ice clouds that offer critical insights into mesospheric dynamics during polar summer
- The CIPS instrument aboard the AIM satellite reveals intricate PMC structures, where a feature is classified as a front only if it shows a sharp boundary between cloudy and clear regions, with significantly higher albedo along the boundary compared to the adjacent cloudy area
- This study presents a Southern Hemisphere case study of a confirmed PMC front observed on December 15, 2009
- To investigate the surrounding mesospheric environment, we use coincident temperature profiles from SABER instrument aboard the TIMED satellite, focusing on the presence of temperature inversion layers (ILs)
- To assess the influence of gravity waves (GWs) on front formation:
 - We examine zonal wind and geopotential height fields from MERRA-2 at 450 hPa
 - We perform ray tracing simulations using GROGRAT to track wave propagation from the troposphere to the mesosphere using WACCM data

2. SH PMC Front Statistics

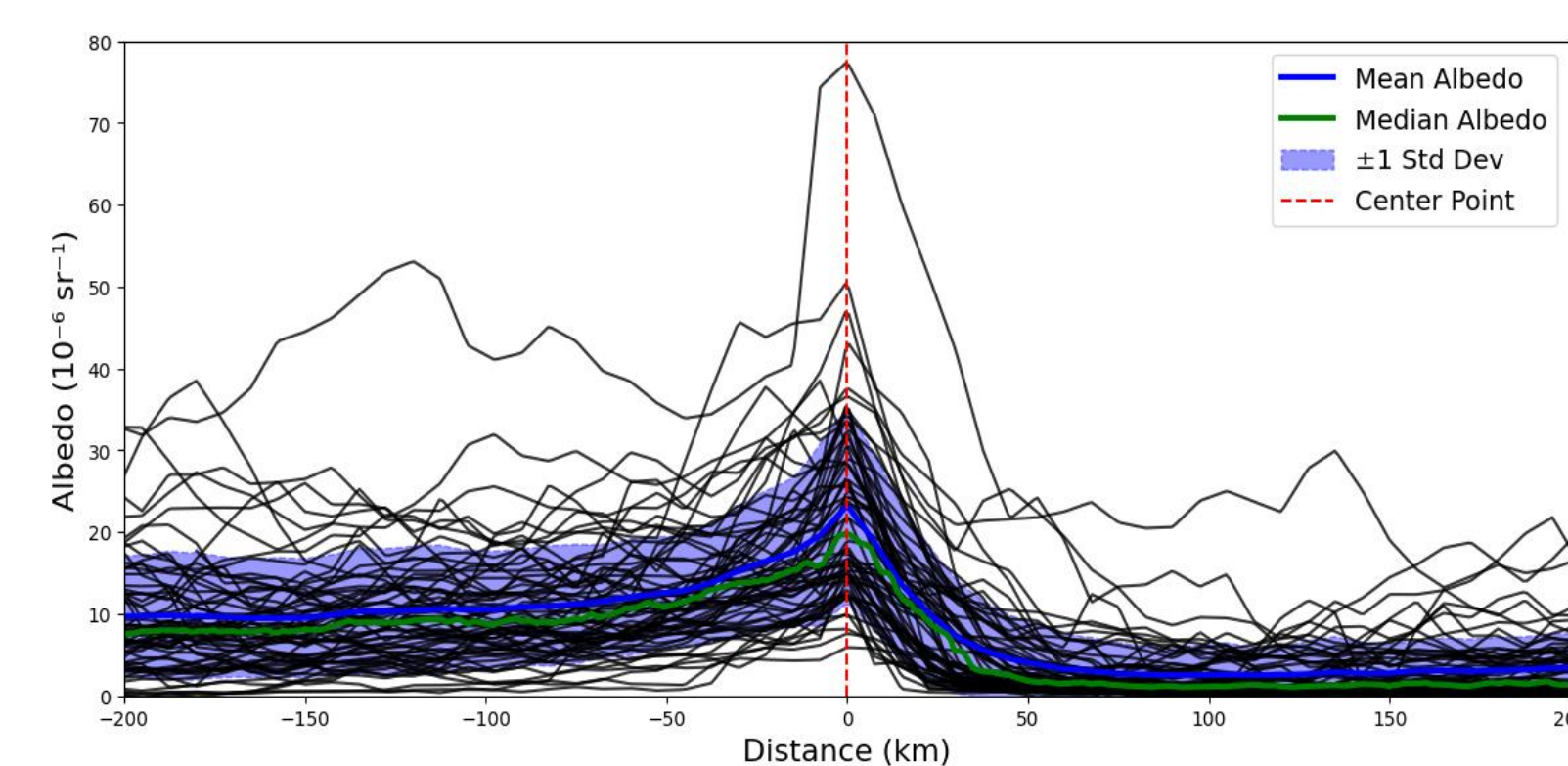


Figure 1: Transects of cloud albedo across all the identified front structures. The distance from the peak albedo at zero km is positive in the mostly clear region and negative in the cloudy region.

The geographic distribution of 65 PMC fronts across 15 seasons shows random appearance poleward of 60°S and spanning all longitudes except between 210°E and 240°E

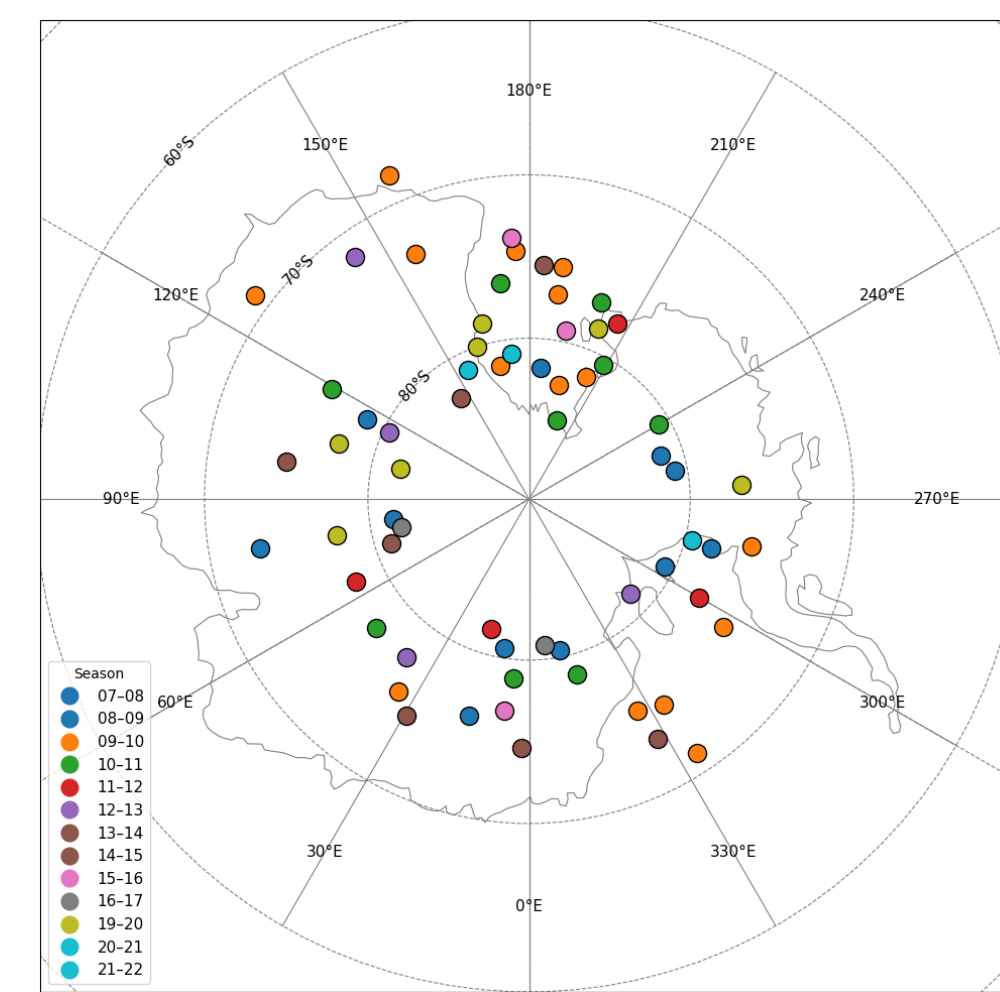


Figure 2: Location of the identified front structures in the SH 2007-2022 PMC Seasons

At the boundary (0 km), the mean and median albedo are $22.98 \pm 11.95 \times 10^{-6} \text{ sr}^{-1}$ and $19.73 \times 10^{-6} \text{ sr}^{-1}$, respectively; it drops approximately 20% in the cloudy region and 80% in the mostly clear region at 100 km from the front

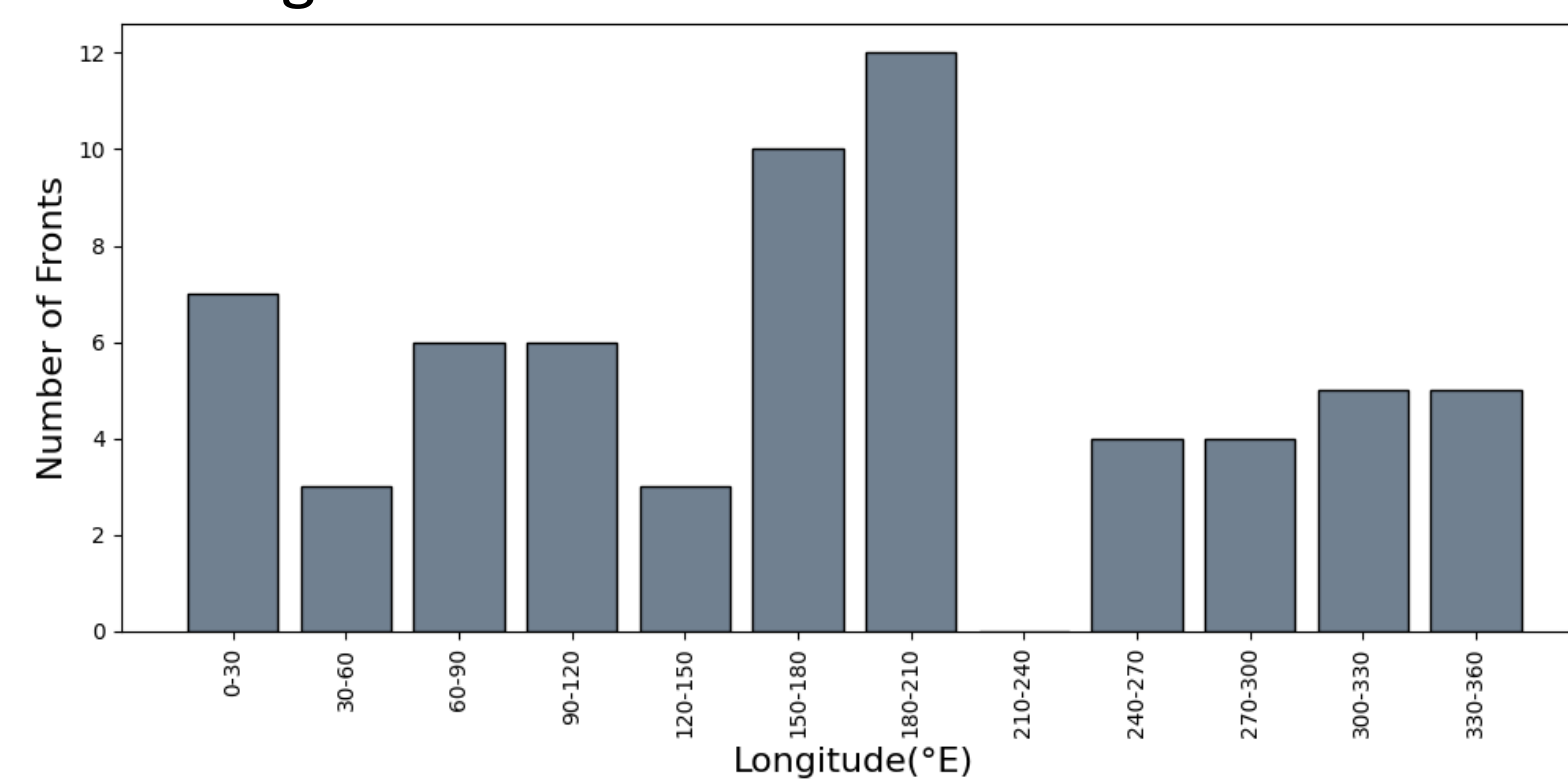


Figure 3: Number of fronts observed in 30° longitude bins in all seasons

Figure 3 shows that most PMC fronts were observed between 180°–210°E, with none between 210°–240°E. To determine if this pattern was due to actual front occurrence or higher cloud coverage, Figure 4 analyzes the ratio between fronts and cloud frequency confirming that more fronts occurred in 180°–210°E even after accounting for cloud abundance. Similarly, more fronts were observed in season 2009-10 irrespective of cloud frequency as we see in figures 5 and 6

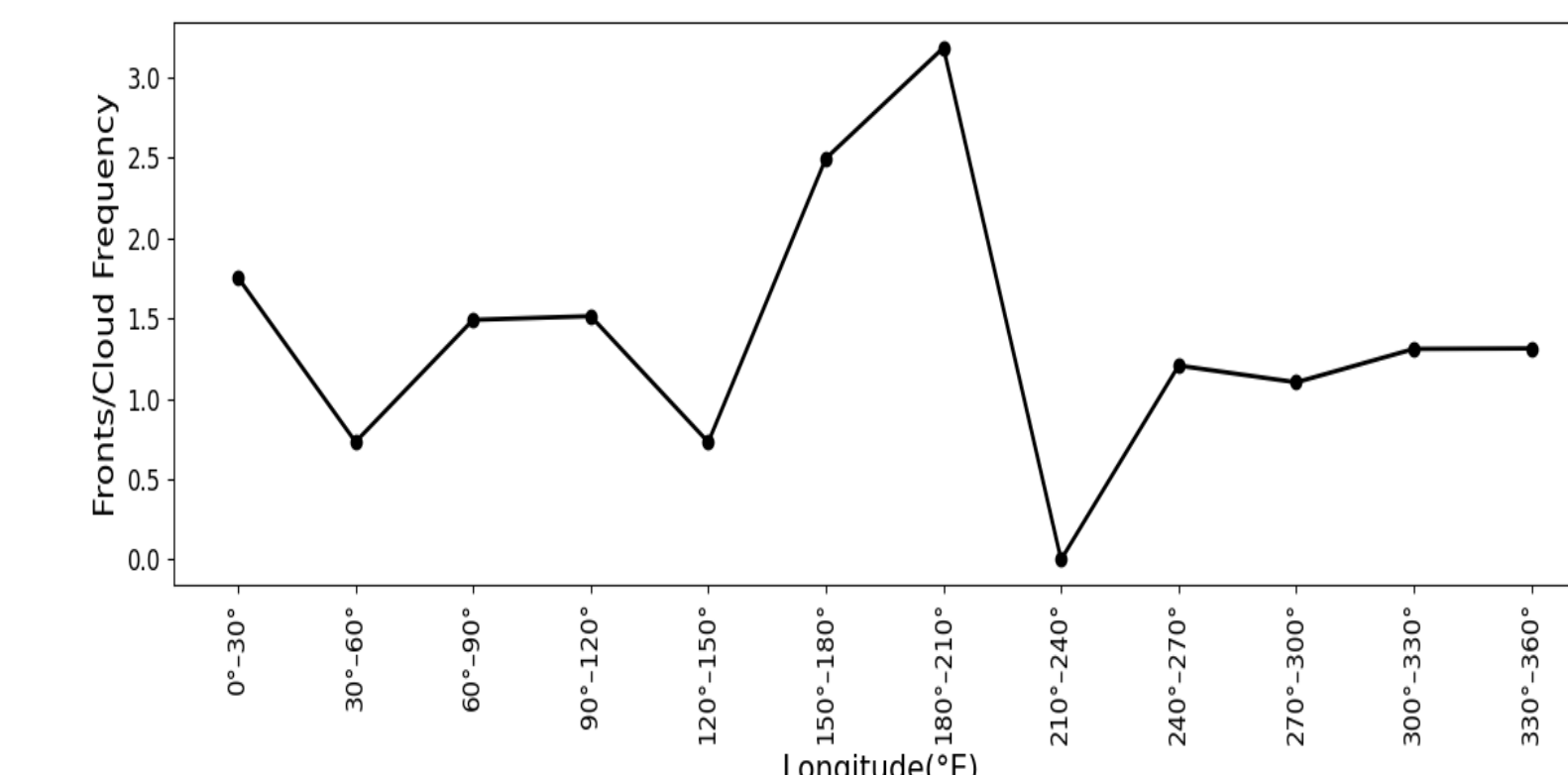


Figure 4: The ratio of number of fronts to the average cloud frequency per longitude bins in all seasons

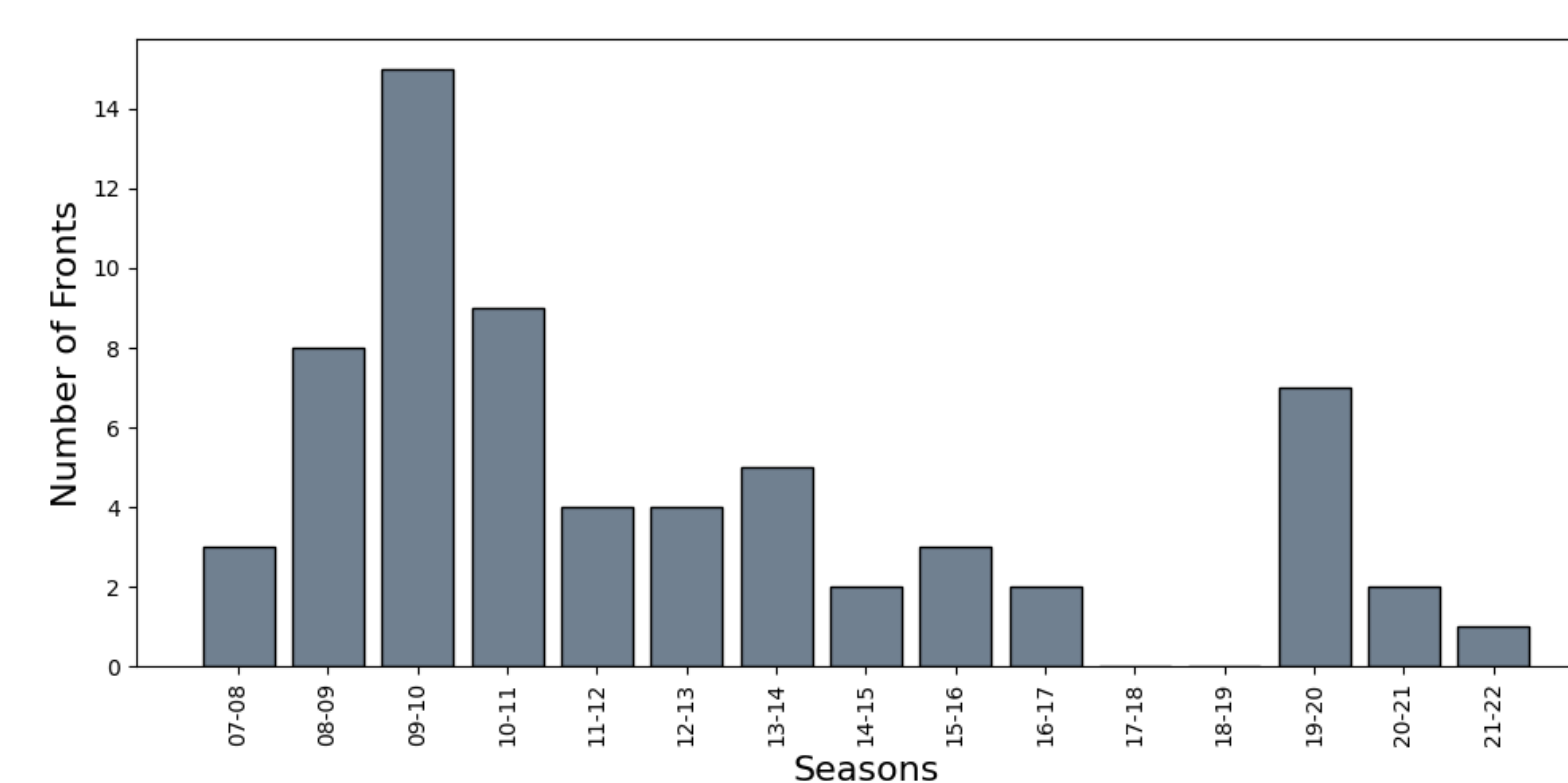


Figure 5: Number of fronts observed per PMC seasons

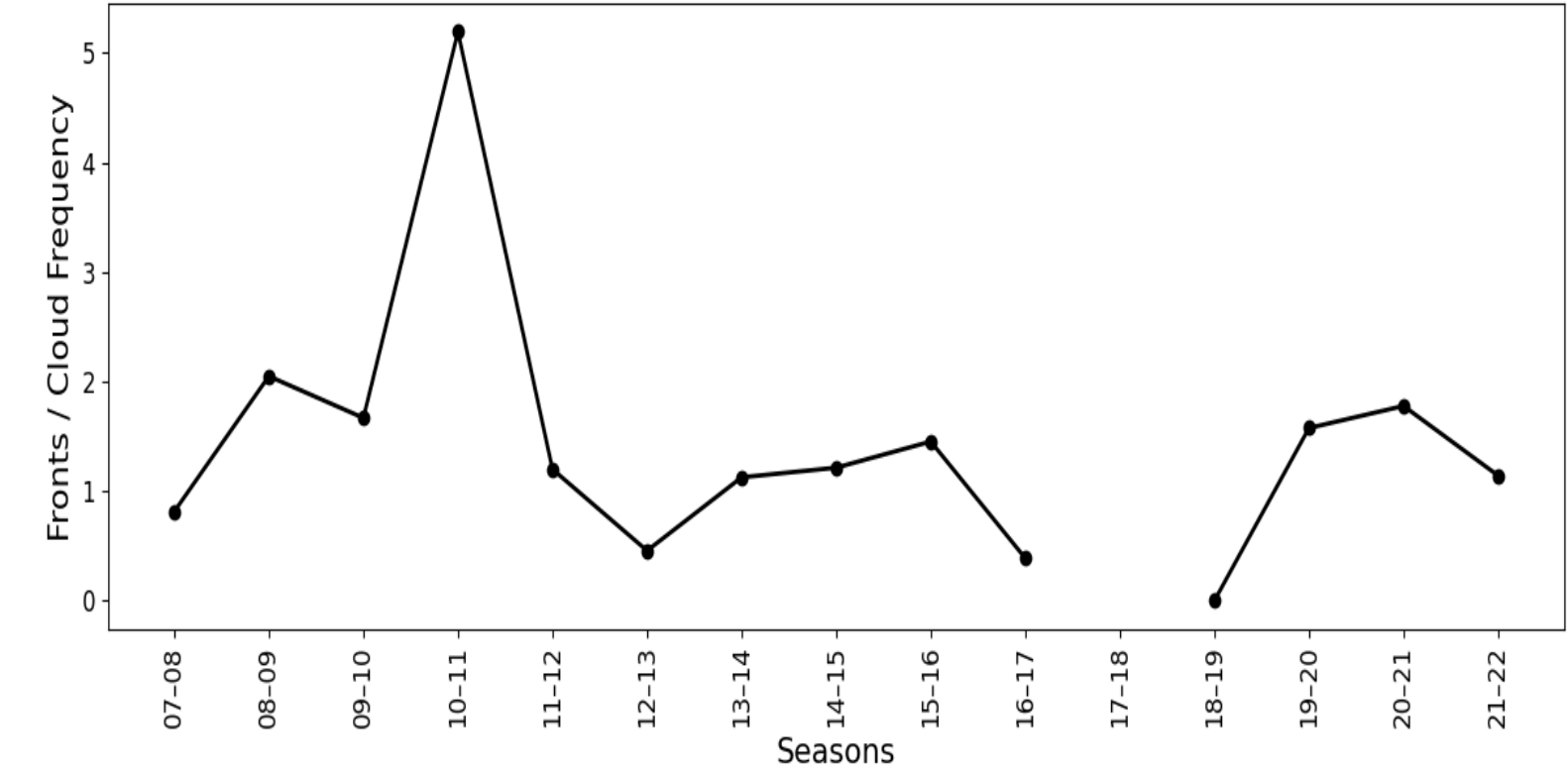


Figure 6: The ratio of number of fronts to the average cloud frequency per PMC seasons

3.1 PMC Front Case Study

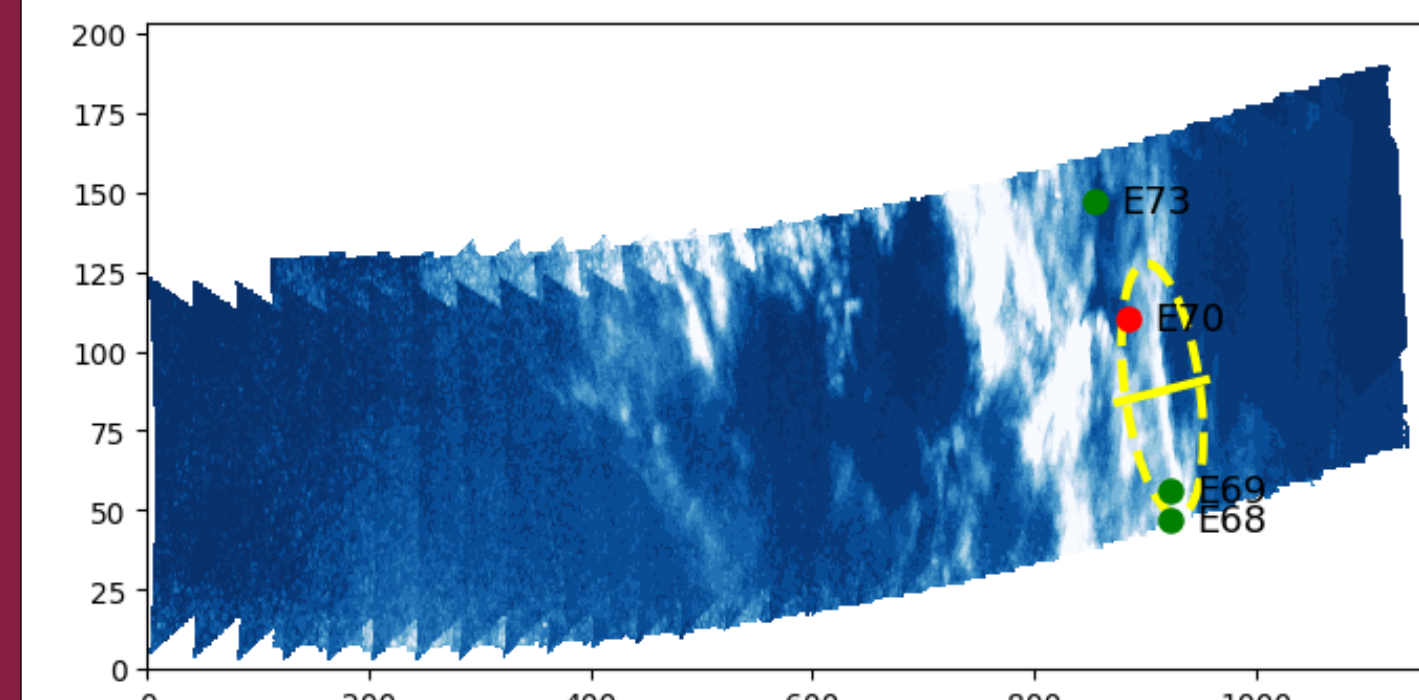


Figure 7: Scan across a PMC front structure as observed by CIPS (highlighted in yellow) on 15 December 2009 and SABER near-coincident (red dot) and neighboring events (green dots)

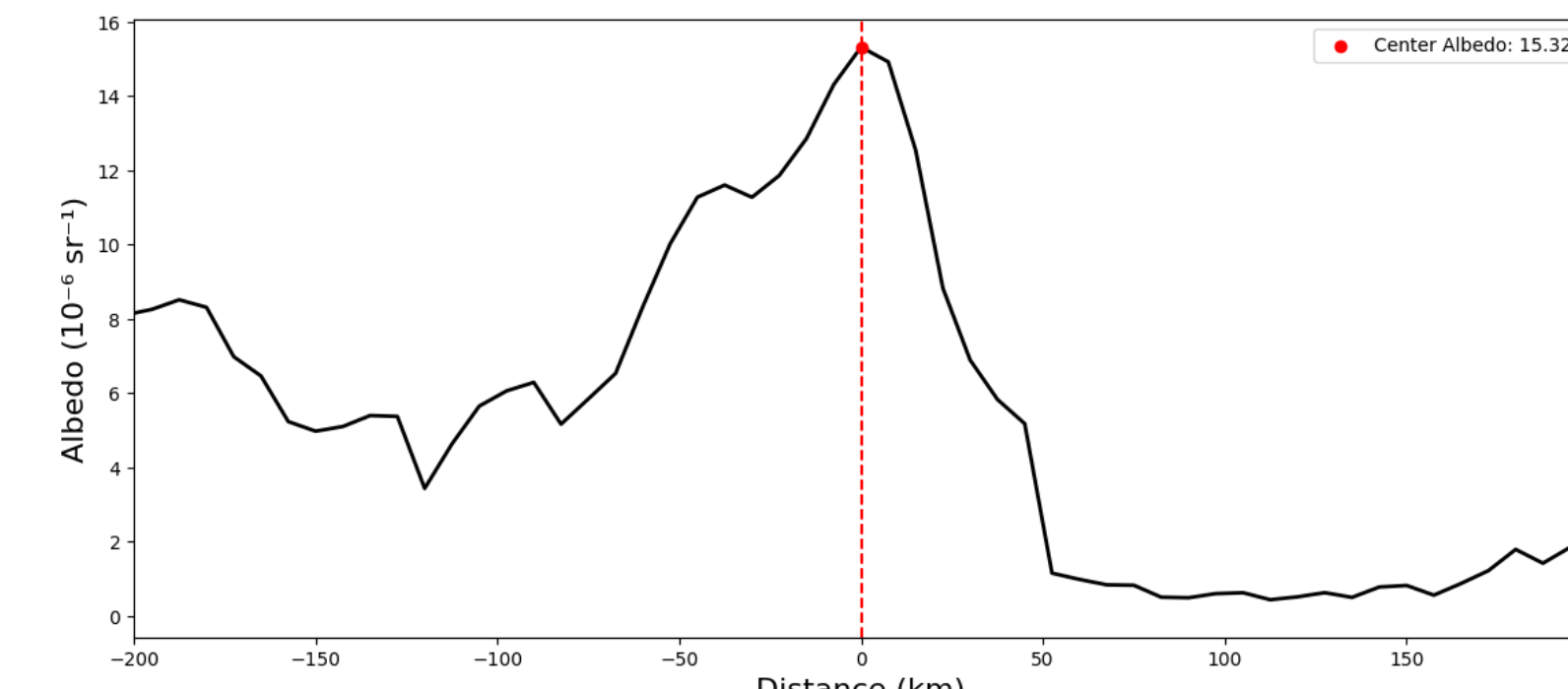


Figure 8: Albedo as a function of distance along the transect (solid yellow line in PMC image)

We examine a randomly selected PMC front structure from December 15, 2009. The CIPS albedo image shows a well-defined front (highlighted in yellow) with SABER near-coincident and neighboring events marked. The corresponding albedo transect reveals a sharp peak ($15.32 \times 10^{-6} \text{ sr}^{-1}$) at the front boundary, followed by a rapid drop revealing the characteristic of a distinct PMC front.

3.2 Mesospheric Conditions Analysis

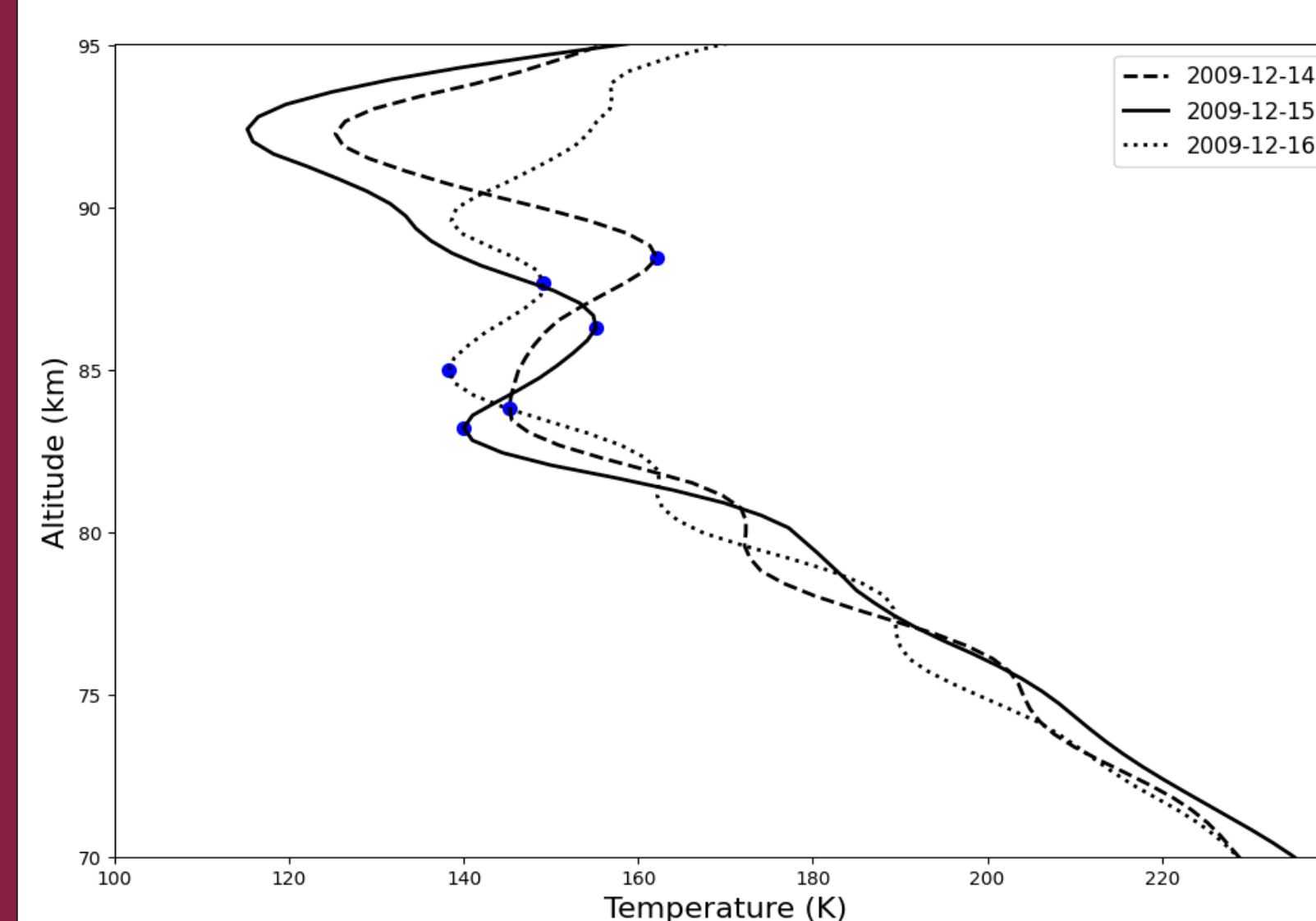


Figure 9: SABER temperature profiles for measurements near-coincidence with the front observed in SABER data on December 15, 2009 (solid line), as well as for the preceding and following days (dashed lines)

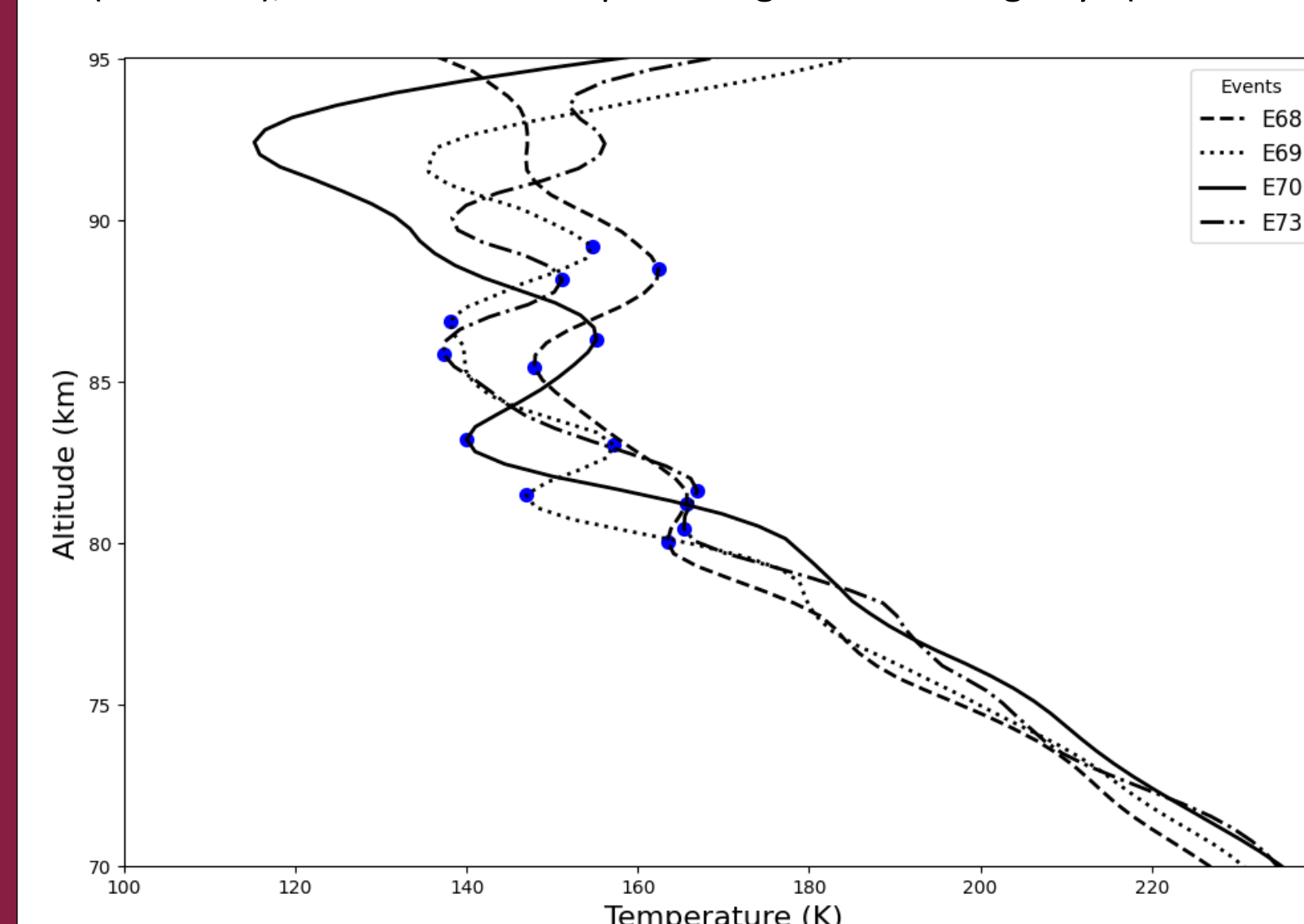


Figure 10: SABER temperature profiles for events E68-E70 and E73. The blue dots denote the peak and bottoms of inversion layers within 80 to 90 km.

Characteristics	2009-12-14	2009-12-15	2009-12-16
Z_{peak} (km)	88.4	86.3	87.7
T_{peak} (K)	162.1	155.2	149.1
Amplitude (K)	16.9	15.2	10.9
Depth (km)	4.6	3.1	2.7
Topside lapse rate (K/km)	11.6	6.9	5.9
Bottom side gradient (K/km)	4	5.2	4.5
Saturation ratio	0.5	2.3	1.4

Table 1: Characteristics of inversion layers between 80 and 90 km observed in SABER temperature profiles near-coincident with the observed front and on other days.

Characteristics	E68	E69	E70	E73
Z_{peak} (km)	88.5	89.2	86.3	88.1
T_{peak} (K)	162.4	154.6	155.2	151.2
Amplitude (K)	14.5	16.5	15.2	13.9
Depth (km)	3.1	2.3	3.1	2.3
Topside lapse rate (K/km)	5.8	8.8	6.9	7.4
Bottom side gradient (K/km)	5.3	7.7	5.2	6.7
Saturation ratio	0.11	1.2	2.3	1.8
Albedo (10^{-6} sr^{-1})	9.7	8.4	1.9	1.4

Table 2: Characteristics of significant inversion layers (>12K) between 80 and 90 km observed in SABER temperature profiles and CIPS albedo for events E68-E70 and E73.

4. Conclusions and Future Work

- SABER profiles revealed temperature inversion layer near the front location, suggesting thermal structuring in the mesosphere may support front formation
- Zonal wind and geopotential height fields identified dynamically active regions likely to generate gravity waves
- GROGRAT simulations show that in general waves with higher phase speeds and shorter wavelength are more likely to reach high latitude mesosphere
- Extend the analysis to more front events across multiple seasons for robust assessment of front formation conditions
- Investigate the combined influence of gravity waves, planetary waves, and tides on PMC front structures to develop a more comprehensive understanding of mesospheric dynamics

3.3. Gravity Wave Analysis

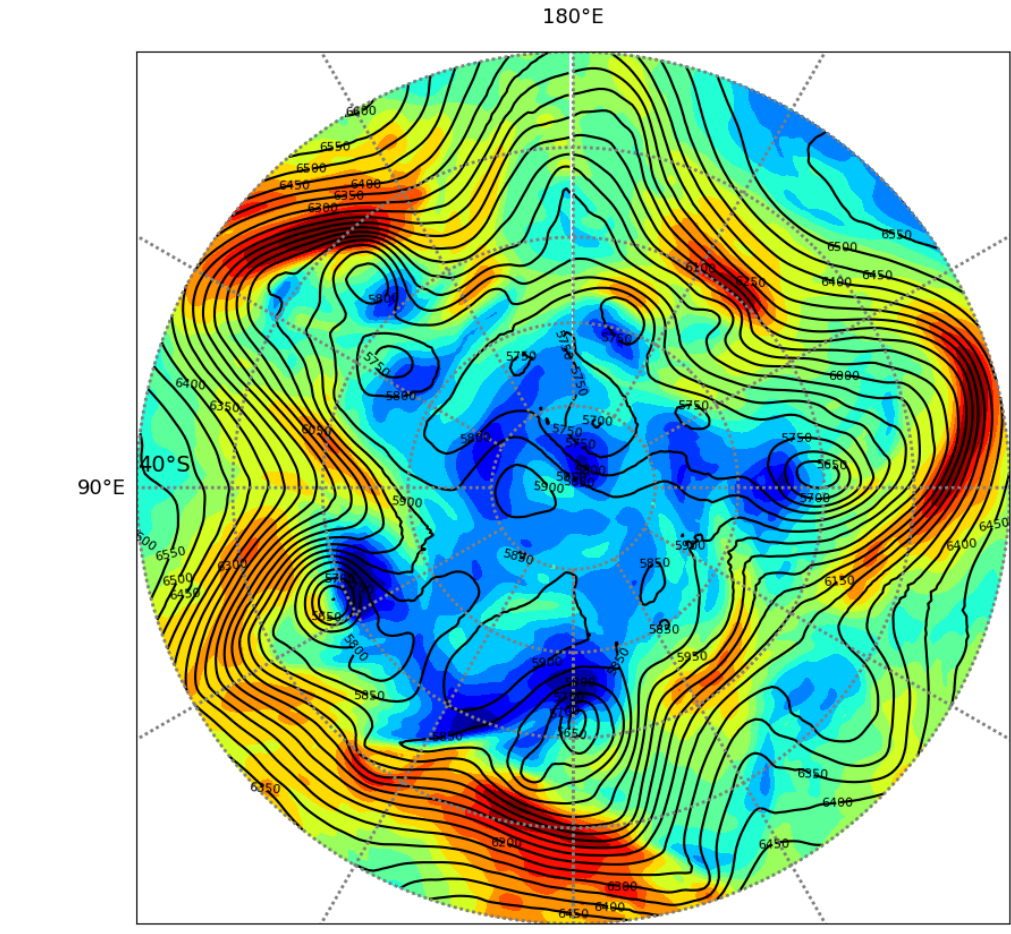


Figure 10: Zonal wind and geopotential height at 450 hPa on 15 December, 2009 at 18 UT i.e. closest to the observed front on the same day

- Figure 10 shows sharp wind speed variations near geopotential height troughs and ridges, identifying dynamically active regions likely to generate GWs. These span from 0 to 360 °E
- To examine GW propagation, we performed GROGRAT ray-tracing simulations using WACCM background data. A total of 800 rays per wavelength-speed combination were launched from troposphere to trace wave trajectories
- Figure 11 shows the summary of the simulations which reveals that higher phase speeds lead to more GWs reaching the mesosphere

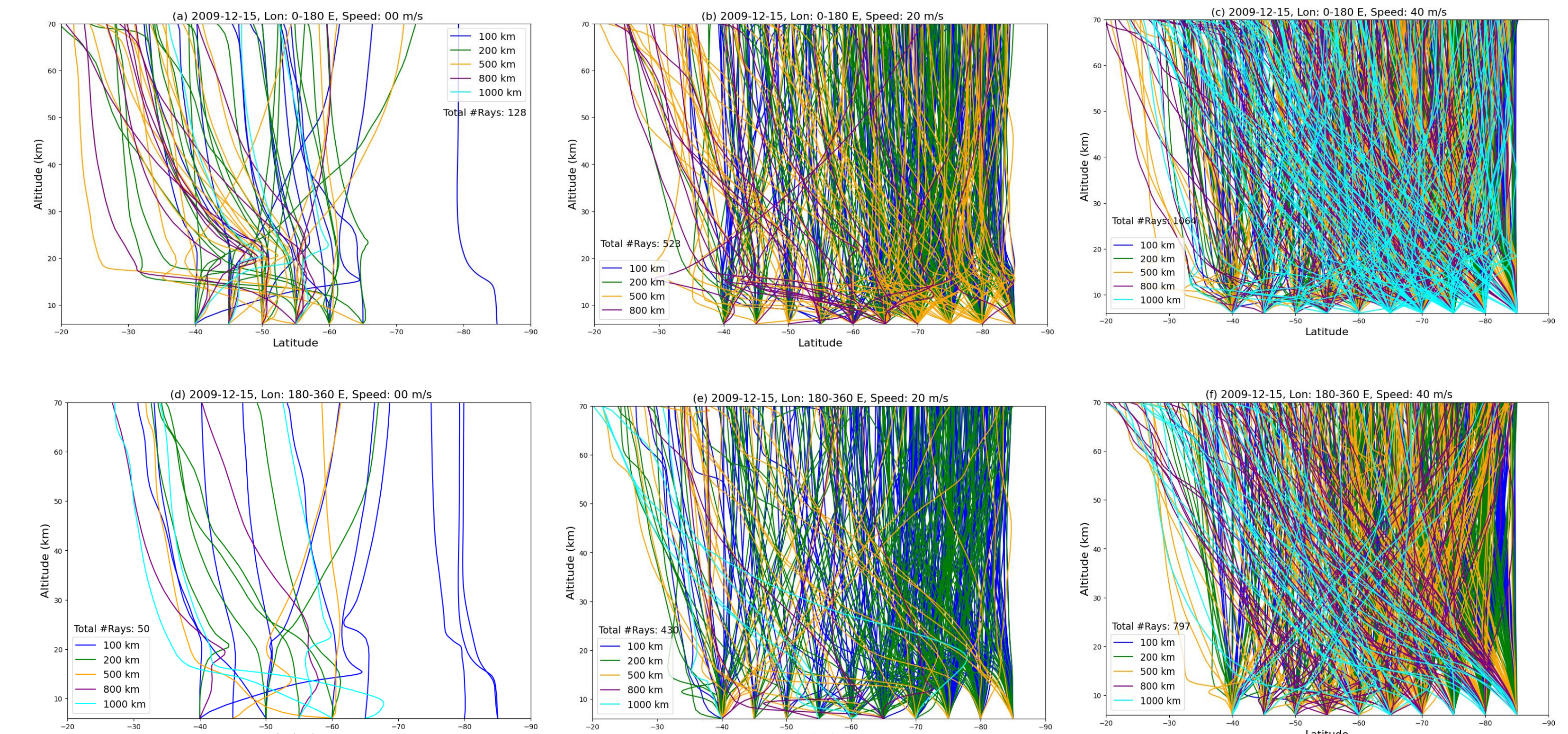


Figure 11: GW raypaths for phase speeds of (a, d) 0 m/s, (b, e) 20 m/s, and (c, f) 40 m/s that reached mesosphere. Upper panels (a-c) show the number of propagating waves within 0 to 180°. Lower panels (d-f) show the number of propagating waves within 180 to 360°. The blue, green, orange, purple and cyan colors indicate GWs with horizontal wavelengths of 100, 200, 500, 800 and 1000 km respectively.

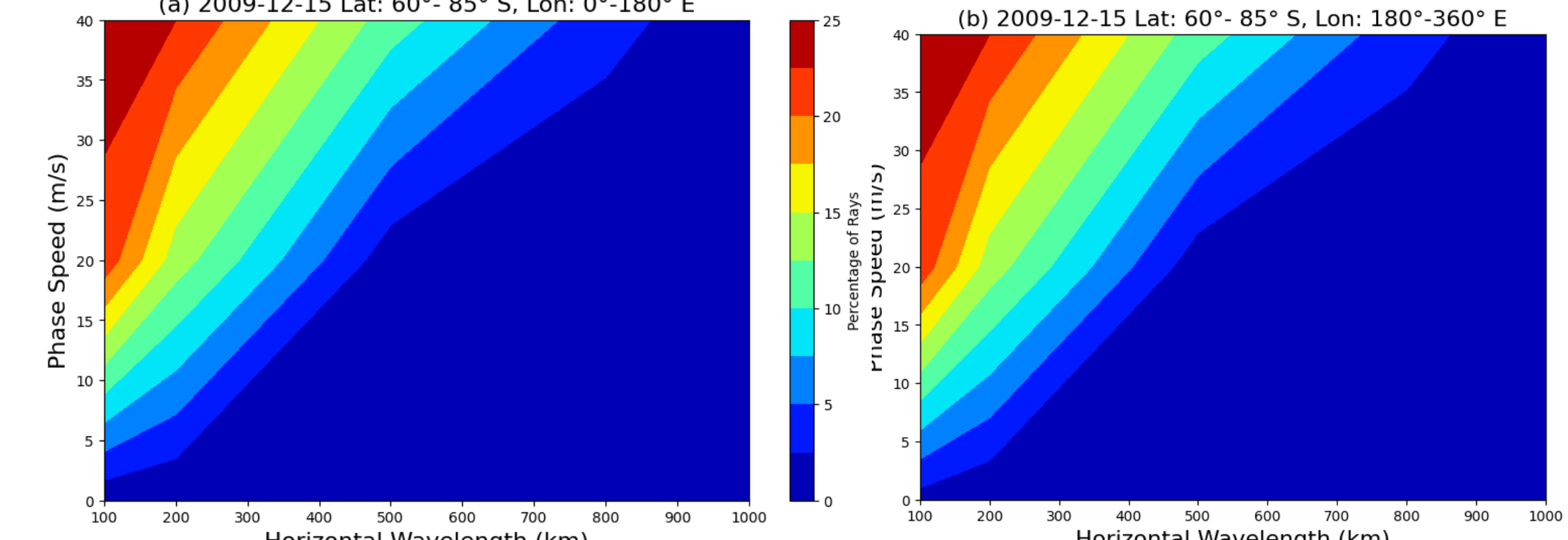


Figure 12: Percentage of GWs originating in troposphere that reach high latitude (60-85°S) mesosphere in (a) 0-180°E and (b) 180-360° E

Figure 12 exhibits that in general irrespective of vertical and oblique propagation, waves with shorter wavelengths and higher phase speeds have higher probability of reaching the high latitude mesosphere

5. Acknowledgement

We acknowledge funding from NSF Award # 2149483- CEDAR: Characteristics of Front Like structures in Polar Mesospheric clouds

6. References

1. Thurairajah, B., Cullens, C. Y., Harvey, V. L., & Randall, C. E. (2024). A Statistical study of polar mesospheric cloud fronts in the northern hemisphere. *Journal of Geophysical Research: Atmospheres*, 129, e2024JD041502
2. Thurairajah, B., Cullens, C. Y., Siskind, D. E., Hervig, M. E., & Bailey, S. M. (2020). The role of vertically and obliquely propagating gravity waves in influencing the polar summer mesosphere. *Journal of Geophysical Research: Atmospheres*, 125(9), e2020JD032495.
3. Alexandre, D. (2021). The influence of obliquely propagating monsoon gravity waves on the polar summer mesosphere (Doctoral dissertation, Virginia Tech). Virginia Tech Libraries. <https://techworks.lib.vt.edu/items/4ce0517d-4294-41ef-9bbf-ae929fb10de4>